Acta Pharmaceutica Sinica B 2020;10(2):276–288

Chinese Pharmaceutical Association
Institute of Materia Medica, Chinese Academy of Medical Sciences

Acta Pharmaceutica Sinica B

www.elsevier.com/locate/apsb
www.sciencedirect.com

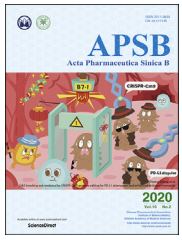

ORIGINAL ARTICLE

A novel $S1P_1$ modulator IMMH002 ameliorates psoriasis in multiple animal models

Jing Jin[a,*,†], Nina Xue[a,†], Yuan Liu[b], Rong Fu[a], Mingjin Wang[a], Ming Ji[a], Fangfang Lai[a], Jinping Hu[a], Xiaojian Wang[a], Qiong Xiao[a], Xiaoying Zhang[a], Dali Yin[a], Liping Bai[c], Xiaoguang Chen[a,*], Shuan Rao[b,*]

[a]*State Key Laboratory of Bioactive Substances and Functions of Natural Medicines, Institute of Materia Medica, Chinese Academy of Medical Sciences, Peking Union Medical College, Beijing 100050, China*
[b]*Department of Thoracic Surgery, Nanfang Hospital, Southern Medical University, Guangzhou 510515, China*
[c]*State Key Laboratory of Quality Research in Chinese Medicine, Macau Institute, for Applied Research in Medicine and Health, Macau University of Science and Technology, Taipa, Macau SAR 999078, China*

Received 19 June 2019; received in revised form 16 October 2019; accepted 21 October 2019

KEYWORDS

$S1P_1$;
$S1P_1$ agonist;
IMMH002;
Lymphocyte;
Psoriasis

Abstract Psoriasis is characterized by abnormal proliferation of keratinocytes, as well as infiltration of immune cells into the dermis and epidermis, causing itchy, scaly and erythematous plaques of skin. The understanding of this chronic inflammatory skin disease remains unclear and all available treatments have their limitations currently. Here, we showed that IMMH002, a novel orally active $S1P_1$ modulator, desensitized peripheral pathogenic lymphocytes to egress signal from secondary lymphoid organs and thymus. Using different psoriasis animal models, we demonstrated that IMMH002 could significantly relieve skin damage as revealed by PASI score and pathological injure evaluation. Mechanistically, IMMH002 regulated $CD3^+$ T lymphocytes re-distribution by inducing lymphocytes' homing, thus decreased T lymphocytes allocation in the peripheral blood and skin but increased in the thymus. Our results suggest that the novel $S1P_1$ agonist, IMMH002, exert extraordinary capacity to rapidly modulate T lymphocytes distribution, representing a promising drug candidate for psoriasis treatment.

*Corresponding authors.
E-mail addresses: rebeccagold@imm.ac.cn (Jing Jin), chxg@imm.ac.cn (Xiaoguang Chen), raoshuan1@smu.edu.cn (Shuan Rao).
[†]These authors made equal contributions to this work.
Peer review under responsibility of Institute of Materia Medica, Chinese Academy of Medical Sciences and Chinese Pharmaceutical Association.

https://doi.org/10.1016/j.apsb.2019.11.006

1. Introduction

Psoriasis is a chronic immune system disorder with an approximately 2%−3% prevalence worldwide. The pathophysiology of psoriasis is characterized by abnormal proliferation of keratinocytes and infiltration of immune cells into the dermis and epidermis, inducing itchy, scaly, erythematous plaques of skin[1]. Various comorbidities, including psoriatic arthritis, cardiovascular and psychiatric complications, have been associated with psoriasis, which severely impact the quality of life[2]. Currently, most of clinical available drugs against psoriasis can only relieve the symptoms with different limitations or side effects, thus development of new generation of anti-psoriasis drugs with sustained efficacy and improved safety is utmost demanded[3−5].

Sphingosine-1-phosphate receptor subtype 1 ($S1P_1$) is the most well-defined subtype among five sphingosine-1-phosphate receptors (sphingosine-1-phosphate receptor subtypes 1−5, $S1P_{1-5}$)[6,7]. It has been widely recognized that $S1P_1$ is essential for lymphocyte recirculation and responsible for lymphocyte egress from secondary lymphatic organ (SLO) and thymus. Deletion of $S1P_1$ in mouse hematopoietic cells results in absence of T cells in the periphery blood as the essential signal in regulating mature T cells to exit from SLO and thymus is missing[6,8,9]. Since $S1P_1$ is indispensable for lymphocyte trafficking and immune system regulation, it has been actively studied as a promising therapeutic target for autoimmune diseases which are usually correlated with lymphocyte dysfunction and infiltration.

Till now, the molecular mechanisms underlying psoriasis progression are still unclear despite recent evidences highlighted that the infiltration of lymphocytes, particularly Th17 cells, as well as elevated cytokines, triggered epidermal hyperplasia, and then induce psoriatic phenotype[10−12]. It is widely recognized that inhibiting the accumulation of pathogenic lymphocytes in the circulation and infiltration into the skin legion by targeting $S1P_1$ represents an emerging therapeutic avenue for psoriasis treatment. For example, fingolimod (FTY720/Gilenya, Novartis), a multifunctional S1P receptors modulator ($S1P_1$, $S1P_3$, $S1P_4$ and $S1P_5$), has been proved effective in many animal models of autoimmune diseases, such as experimental autoimmune encephalitis, rheumatoid arthritis, and systemic lupus erythematosus[13−15]. It was approved by the U.S. Food and Drug Administration (FDA) for treating relapsing-remitting multiple sclerosis (RMS) since 2010[16]. Another similar compound, ponesimod, has successfully completed phaseIIclinical trials for the treatment of moderate-to-severe chronic plaque psoriasis and showed great efficacy, safety and tolerability for psoriasis patients[17,18]. As a more specific S1P receptor modulator, Syl930 alleviates inflammation in sodium dodecyl sulfate (SDS)-induced mouse skin irritation[19].

A promising drug candidate of $S1P_1$ agonist with high efficacy and good safety, IMMH002, was previously reported in our group[20]. IMMH002 retained the key polar head group of FTY720 with inserted aromatic substituent in order to increase its structural rigidity, thus increasing the selectivity to $S1P_1$ receptor. It is a novel $S1P_1$ modulator which can be further converted to its active phosphorylated form (IMMH002-P) *in vivo*, and exhibits improved receptor selectivity and optimized pharmacokinetic properties compared to FTY720[21]. In this study, IMMH002 was demonstrated to induce significant $S1P_1$ receptor internalization and a rapidly reversible reduction of periphery blood lymphocytes (PBLs) in rats without any side effects such as bradycardia, a complication usually occurred in preculinaryand clinical studies of FTY720. Furthermore, IMMH002 were shown relieving SDS-induced mouse skin irritation and alleviating propranolol-induced damage in a guinea pig model of psoriasis. Moreover, IMMH002 effectively decreased T-lymphocyte infiltration in skin legion in the imiquimod (IMQ)-induced mouse psoriasis model.

2. Materials and methods

2.1. Cell lines

The transfected Chinese hamster ovary-K1 (CHO-K1) Gαqi5 cells with stable $S1P_1$ expression, $hS1P_1$-CHO, was obtained from the Multispan, Inc. (Hayward, CA, USA). Cells were maintained in DMED/F12 medium supplemented with 10 μg/mL puromycin, 250 μg/mL hygromycin and 10% fetal bovine serum (FBS, GIBCO, Grand Island, NY, USA).

2.2. Animals

Age matched, 6−8 weeks old male Sprague−Dawley (SD) rats, female/male Kunming (KM) mice and male BALB/c mice were obtained from the Vital River Laboratory Animal Technology Co., Ltd. (Beijing, China). Female Hartley guinea pigs (4−6 weeks old) were obtained from the National Institute for Food and Drug Control (Beijing, China). All rodents used in the study were housed under standardized light- and temperature-controlled conditions with free access to food and water. All experiments were approved by the ethical committee and carried out in accordance with the guidelines of the Committee on Animals of the Institute of Materia Medica, Chinese Academy of Medical Sciences & Peking Union Medical College (Beijing, China).

2.3. Agents

IMMH002, IMMH002-P, FTY720 and FTY720-P were synthesized as previously described methods[22]. Methotrexate (MTX) was obtained from Shanghai XinYi Parmaceutical Co., Ltd. (Shanghai, China). All the compounds were dissolved in dimethyl sulfoxide (DMSO) for *in vitro* analysis. For *in vivo* studies, IMMH002, FTY720 and MTX were dissolved in distilled water and given orally. Control animals received the vehicle only.

2.4. β-Arrestin assay

The β-arrestin assay was performed with DiscoveRx using enzyme fragment complementation with β-galactosidase as the functional reporter. Briefly, PathHunter CHO-K1-EDG1($S1P_1$) cells, EDG3($S1P_3$) cells, EDG5($S1P_2$) cells, EDG6($S1P_4$) cells and EDG8($S1P_5$) cells were separately seeded in a total volume of 20 μL into white walled, 384-well microplates and incubated at 37 °C overnight. Five μL of 5 × samples with different concentrations of compounds were added and incubated at 37 °C for 2 or 4 h. Assay signal was generated by a single addition of 12.5 μL of PathHunter detection reagent cocktail, followed by 1 h of incubation at room temperature. Microplates were then read with EnVision (PerkinElmer Company, Shelton, CT, USA) instrument for chemiluminescent signal detection and compound activity was

determined using the CBIS data analysis suite (Chem Innovation, San Diego, CA, USA).

2.5. HTRF-IP1 assay

The homogeneous time resolved fluorescence-IP one (HTRF-IP1) assay was performed by IP-One Tb kit purchased from Cisbio (France). According to the manufacturer's protocols, $hS1P_1$-CHO cells and $hS1P_3$-CHO cells were prepared in 1 × stimulation buffer (containing LiCl) and distributed in 7 μL of suspension with a density of 7×10^4 cells/well in 384-well plates. Then, 7 μL test compounds in different concentrations were added into the assay plate and incubated at 37 °C and 5% CO_2 for 2 h. Meanwhile, a standard curve was generated according to the manufacture's instruction. Next, 3 μL IP1-d2 diluted by 1 × lysis buffer was added into each well followed by 3 μL diluted Ab-Cryp. The plates were incubated at room temperature for 1 h and then recorded with EnVision (PerkinElmer) reader for the detection of absorbance at 665 and 615 nm. The ratio of $\text{absorbance}_{665\ nm}$/$\text{absorbance}_{615\ nm}$ (A_{665}/A_{615}) emissions was then calculated. A standard curve was plotted of ratio (A_{665}/A_{615}) *versus* IP-1 concentrations using non-linear least squares fit. The values were calculated with the standard curve and presented as concentration (nmol/L) of IP-1. The A_{665}/A_{615} value of tested compounds should fall into the linear portion of the standard curve. EC_{50} values were calculated by Graphpad software 5.0 (GraphPad Software Inc, La Jolla, CA, USA).

2.6. Flow cytometry analysis

For the $S1P_1$ internalization assay, $hS1P_1$-CHO cells were incubated for 1 h with 10, 100 and 400 nmol/L FTY720-P and IMMH002-P at 37 °C. Then, cells were washed with ice-cold phosphate-buffered saline and blocked with human IgG for 15 min at room temperature followed by incubation with either 25 μg/mL Phycoerythrin (PE)-conjugated mouse anti-human EDG1/$S1P_1$ IgG2B (R&D systems, Minneapolis, MN, USA) or with PE-conjugated isotype control mouse IgG2B (R&D systems) for 1 h at room temperature. Cells were washed and subjected to flow cytometry measurements using 10,000 viable cells per sample. The percentage of internalization of $S1P_1$ (%) was calculated as Eq. (1):

$$\text{Percentage of internalization of } S1P_1\ (\%) = (\text{Fluorescent intensity of solvent control} - \text{Fluorescent intensity of compounds})/(\text{Fluorescent intensity of solvent control} - \text{Fluorescent intensity of isotype control}) \times 100 \quad (1)$$

For the *in vivo* assay, single-cell suspensions of spleen and thymus, as well as peripheral blood, were prepared as previously described[23]. Single-cell suspensions were blocked with nonspecific Fc binding with anti-mouse CD16/32 (clone 2.4G2, eBiosciences, San Diego, CA, USA) and labeled with anti-CD3 for T cells; anti-CD11c, anti-CD11b for conventional dendritic cells; anti-CD11c, anti-CD11b and anti-IA/IE for mature conventional dendritic cells; anti-CD11c, anti-CD45R for plasmacytoid dendritic cells; anti-CD11c, anti-CD45R and anti-IA/IE for mature plasmacytoid dendritic cells. Data were acquired on a FACS Calibur cytometer (Becton Dickinson, East Rutherford, NJ, USA) and analyzed with FlowJo software 9.0 (TreeStar Inc., Ashland, OR, USA).

2.7. Peripheral blood lymphocytes (PBLs) determination after drug treatment

The rats were distributed randomly. Twenty μL blood samples were collected from the tail vein and measured by the MEK-7222K type blood cell analyzer (Nihon Kohden, Japan) with the baseline PBLs level prior to administration (0 h). Then, rats were administrated orally with compounds (0.3, 1, 3 mg/kg IMMH002, and 3 mg/kg FTY720) and vehicle, respectively. The PBLs levels were monitored at 2, 4, 8, 12, 24, 72, 96, 144 and 168 h post administration ($n = 5$).

2.8. Heart rate measurement

The basic heart rates were measured using the intelligent non-invasive blood pressure measurement meter-mice instrument (Softron, Japan). The rats were then administrated with 10 mg/kg IMMH002, 10 mg/kg FTY720 and vehicle, respectively. The heart rates were measured at 2, 4, 8, 12, 24 and 48 h post administration ($n = 5$).

2.9. SDS-induced acute skin irritation and inflammation mouse model

A total of 88 female KM mice were involved in this study. The back hair was removed and 200 μL 15% SDS solution were added onto the hairless area, once a day for 7 days. On Day 8, mice were orally administered with vehicle, 0.3, 0.6, 1.2 and 2.4 mg/kg IMMH002, 1 mg/kg FTY720 or 1.5 mg/kg MTX for 10 days. The mice in control group received vehicle only. On Day 18, all mice were sacrificed and the treated area of back skin was dissected to assess the thickness using a tape measure and fixed in 4% paraformaldehyde followed by histological analysis ($n = 11$).

2.10. Propranolol-induced guinea pig psoriasis like skin lesion

The auricle dorsal surfaces of guinea pigs (female, 250−400 g) were treated with 5% propranolol in emulsifying ointment, twice per day for 3 weeks. The treated animals were then administered with vehicle, IMMH002 (0.3, 0.6, 1.2 and 2.4 mg/kg) or FTY720 (1 mg/kg) once a day and 1 mg/kg MTX twice a week for 2 weeks. The control animals were challenged with emulsifying ointment, twice per day for 3 weeks and received vehicle once a day for 2 weeks. Ear specimens of animals were randomly obtained at the end of the experiment, fixed in 4% paraformaldehyde, and embedded in paraffin. Five μm thick sections were prepared and followed by hematoxylin/eosin analysis. The epidermal thickness was measured ($n = 8$) by Image-Pro Plus 6.0 (Media Cybernetics, Buckinghamshire, UK).

2.11. IMQ-induced mouse psoriasis-like disease model

The mouse model of IMQ-induced psoriasis-like lesions was established as previously reported. A total of 80 female BALB/c mice were used in this study. Except for 10 mice in control group, the left 70 mice were treated with 50 mg of Aldara (5% IMQ cream; 3M Pharmaceuticals, Saint Paul, MN, USA) for 7 consecutive days in a daily fashion (Days 0−6) on the shaved back skin. One hour before IMQ treatment, mice were orally administered with vehicle, 0.3, 0.6, 1.2 and 2.4 mg/kg IMMH002, 1 mg/kg FTY720 or 1.5 mg/kg MTX from Day 1 to Day 6, except on Day 0. To evaluate the severity of inflammation of the back skin, a psoriasis area and severity index

(PASI) was analyzed from Day 1 to Day 6. Mice were assessed individually by evaluating erythema, scaling and thickening on a scale from 0 (no alteration) to 4 (very distinct alteration), respectively. These three individual assessments were added to generate accumulative score from 0 to 12.24 h after the last IMQ treatment, mice were sacrificed by cervical dislocation and back skin samples were isolated and fixed in 4% paraformaldehyde followed by histological assessment ($n = 10$).

2.12. Histology and immunohistochemistry (IHC) staining

Skin samples were embedded in paraffin and 5 μm thick sections were cut for hematoxylin/eosin staining and evaluated in a double-blind manner. For the SDS-induced mouse acute skin irritation and inflammation model, the pathological scoring was assessed by evaluating epidermal thickening, fibroplasia, inflammatory cell infiltration and vasodilatation with a semi-quantitative analysis using established criterion (epidermal thickening: 0 = no thickening, 1 = slightly thickening of 5−7 layers, 2 = moderate thickening of 8−10 layers, 3 = severe thickening of more than 10 layers; fibroplasia: 0 = no fibroplasia, 1 = mild fibroplasia of less than 1/3 dermis thickness, 2 = moderate fibroplasia of 1/3−2/3 dermis thickness, 3 = severe fibroplasia of more than 2/3 dermis thickness; inflammatory cell infiltration: 0 = no inflammatory cell infiltration, 1 = mild inflammatory cell infiltration, 2 = moderate inflammatory cell infiltration, 3 = severe inflammatory cell infiltration with diffuse lesions; vasodilatation: 0 = no vasodilatation in dermis, 1 = mild vasodilatation in dermis, 2 = moderate vasodilatation in dermis with limited area, 3 = severe and diffuse vasodilatation in dermis). For the IMQ-induced mouse psoriasis model and the propranolol-induced guinea pig psoriasis model, the pathology score was evaluated as follows (Corneous layer) munro's microabscess, 1.5; hyperkeratosis, 0.5; parakeratosis, 0.5−1.5; (Epidermis) lengthening of rete ridges, 0.5−1.5; lack of granular layer, 1; acanthosis, 1; (Dermis) inflammatory cell infiltration, 0.5−1.5; papillary papillae congestion, 1; thinning above papillae, 1.

The immunohistochemistry staining was carried out as previously described[24]. Briefly, sections were de-paraffinized and dehydrated followed by antigen retrieval using hot citrate buffer. Sections were then blocked in 5% normal horse serum and 1% normal goat serum, and then incubated with the anti-proliferating cell nuclear antigen (PCNA) antibody (1:100, Bioss, Woburn, MA, USA) overnight. The ABC Elite Kit and the DAB Kit (Vector, Burlingame, CA, USA) were used to visualize PCNA-positive cells according to the manufacturer's instructions. After immune-peroxidase labeling, the expression of PCNA was assessed by calculating the portion of PCNA-positive cells among every 200 random cells. The images were acquired with an Olympus BX43 microscope and the analysis was performed using Image-Pro Plus 7.2 AMS software (Media Cybernetics Inc., Buckinghamshire, UK).

2.13. Western blot analysis

The skin tissues of mice were lysised with radio immunoprecipitation assay (RIPA) lysis buffer in addition to protein degradation inhibitors. Equal amounts of total protein, determined by BCA protein quantitative reagent (CWBIO), were separated by sodium dodecyl sulphate−polyacrylamide gel electrophoresis (SDS−PAGE) and blotted onto polyvinylidene fluoride (PVDF) membranes. Membranes were first blocked with 5% skimmed milk at room temperature for 2 h then incubated with the anti-CD3 antibody (1:100, Abcam, Cambridge, UK) at 4 °C overnight. Membranes were detected with anti-rabbit IgG−HRP in a standard ECL reaction (Image Quant LAS 4000 mini, GE, Boston, MA, USA) according to the manufacturer's instructions. Densitometry analysis of the band intensity was carried out using Image J software (NIH, Bethesda, MD, USA).

2.14. Targeted protein-chip assay

The targeted protein chip assay was carried out by RayBio^R (Beijing, China). In brief, mice skin samples were isolated and lysed by tissue lysate to get the protein samples. Meanwhile, the multi-protein-chips were pretreated by blocking with 30 μL blocking solution/well at room temperature for 1 h. Next, the prepared samples were incubated in different wells for 45 min followed by incubation with detection antibody for 1 h at room temperature. Subsequently, diluted streptavidin-Cy3 was added and incubated for 1 h at room temperature. After several washes, the protein-chip images were detected by LuxScanTM 10 K Microarray Scanner.

2.15. ELISA assay

Fifty mg back skin tissue of each mouse was isolated and lysed (10 mg tissue per 100 μL tissue lysate, Beijing Solarbio Science & Technology Co., Ltd., Beijing, China) at 4 °C for 30 min. The obtained protein solutions were quantified by BCA protein quantitative kit (Beijing Lablead Biotech Co., Ltd., Beijing, China). Subsequently, the contents of IL-17A of each sample were detected by IL-17A ELISA kit (Neobioscience, Shenzhen, China) according to the manufacturer's protocols. Briefly, 100 μL sample was added to the reaction well and incubated for 90 min at 37 °C. The plate was washed for 5 times and biotinylated antibody working solution was added to the reaction well and incubated for 1 h at 37 °C. Then, the plate was washed for 5 times and 100 μL enzyme conjugate working solution was added to the reaction well, and incubated for 30 min at 37 °C in the dark. One hundred μL of chromogenic substrate was added to each well and incubated for 15 min at 37 °C in the dark. Finally, 100 μL of reaction stop solution was added to each well and detected at OD_{450} by microplate reader (Synergy H1, BioTek, Winooski, VT, USA) immediately.

2.16. Statistical analysis

All values were presented as mean ± standard error. Analysis was performed using unpaired *t*-test (for 2 group analysis) or one-way ANOVA test (for analysis of 3 or more groups).

3. Results

3.1. IMMH002-P activates $S1P_{1/4/5}$ in vitro

Like FTY720, IMMH002 can be transformed to IMMH002-P *in vivo*. The structure of IMMH002 and IMMH002-P are shown in Fig. 1A. The effect of IMMH002 and IMMH002-P on 5 different S1P receptors was first tested using β-arrestin assay. As shown in Table 1, $S1P_1$, $S1P_4$, and $S1P_5$ were significantly activated by IMMH002-P with EC_{50} of 12.4, 19.8 and 29.4 nmol/L, respectively. However, IMMH002-P only showed mild activation effect

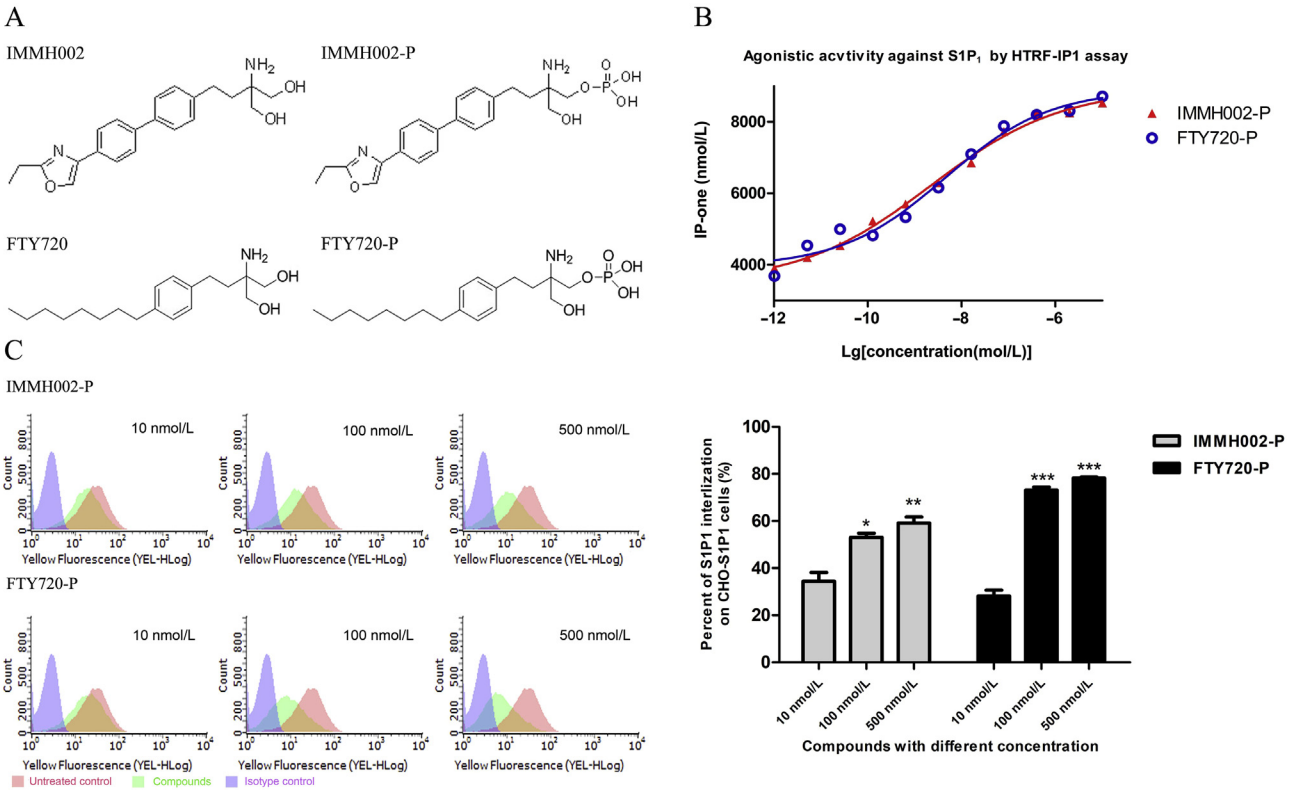

Figure 1 IMMH002-P induces activation and internalization of $S1P_1$. (A) Chemical structures of IMMH002, IMMH002-P, FTY720 and FTY720-P. (B) HTRF-IP1 assay of IMMH002-P and FTY720-P. HTRF-IP1 assay of $S1P_1$ agonists on stably transfected CHO-$S1P_1$ and CHO−$S1P_3$ cells. EC_{50} values are the mean of three to four measurements performed in duplicate. (C) Flow cytometry analysis of $S1P_1$ expression in CHO-$S1P_1$ cell membrane (left panel) and quantification of $S1P_1$ internalization (right panel). $^{*}P \leq 0.05$ group, $^{**}P \leq 0.01$, $^{***}P \leq 0.001$ *vs*. 10 nmol/L group of corresponding compound..

Table 1 The agonistic activity of IMMH002, IMMH002-P and S1P at $S1P_1$−$S1P_5$ by β-arrestin assay.

Compd.	EC_{50} (nmol/L)				
	$S1P_1$ (EDG1)	$S1P_2$ (EDG5)	$S1P_3$ (EDG3)	$S1P_4$ (EDG6)	$S1P_5$ (EDG8)
IMMH002	253.0	>10,000	4,228.7	366.6	291.4
IMMH002-P	12.4	>5,000	>5,000	19.8	29.4
S1P	20.6	103.3	17.7	49.1	30.2

on $S1P_2$ and $S1P_3$ with EC_{50} more than 5000 nmol/L. The pro-drug IMMH002 also showed weak activity on S1P receptors.

3.2. *IMMH002-P induces activation and internalization of $S1P_1$*

In order to further investigate the agonistic activity of IMMH002-P on $S1P_1$, both HTRF-IP1 assay and flow cytometry analysis were performed. As previously reported[25], the HTRF-IP1 assay was an ideal cellular evaluation system to analyze the $S1P_1$ receptor's activation using a GPCR coupled Gq signal transduction. As shown in Fig. 1B, in line with the result of β-arrestin assay, $S1P_1$ was fully activated by IMMH002-P with an EC_{50} of 2.2 nmol/L, which was similar to FTY720-P (EC_{50} = 4.4 nmol/L). Currently, most reported $S1P_1$ agonists are functional inhibitors which decrease the expression of membrane $S1P_1$ by inducing $S1P_1$ internalization[16,26,27]. Therefore, we incubated human $S1P_1$ receptors overexpressed h$S1P_1$-CHO cells with IMMH002-P and determined surface receptor expression levels by flow cytometry anaylsis. Our data showed that 34%, 53% and 59% of total $S1P_1$ receptors were internalized after 1 h incubation of 10, 100 and 500 nmol/L IMMH002-P, respectively (Fig. 1C). Similarly, FTY720-P induced 28%, 73% and 78% internalization of $S1P_1$ receptors at same concentrations, indicating the capacity and mechanism to activate $S1P_1$ of IMMH002-P was comparable to FTY720-P.

3.3. *A single oral administration of IMMH002 dramatically decreases the number of peripheral blood lymphocytes in SD rats*

$S1P_1$ agonists, such as FYT720, KRP203 and SEW2871, can significantly inhibit $S1P_1$-dependent lymphocyte egress from SLO and decrease PBLs, which contribute to their therapeutic effects against many autoimmune diseases[28]. To investigate the effect of IMMH002 on the lymphocytes' circulation, we examined PBLs of SD rats at different time points with a single oral administration of different concentrations IMMH002. PBLs of SD rats decreased rapidly followed by IMMH002 administration and reached the minimum level 12 h after the treatment (Fig. 2), which was similar to FTY720. However, although FTY720 showed a similar lymphopenia effect as IMMH002, the decreased PBLs induced by FTY720 lasted for a much longer period; as one administration of FTY720 could still reduce 26% lymphocyte 1 week later. Moreover, the maximal inhibition ratio of PBLs in SD rats treated with

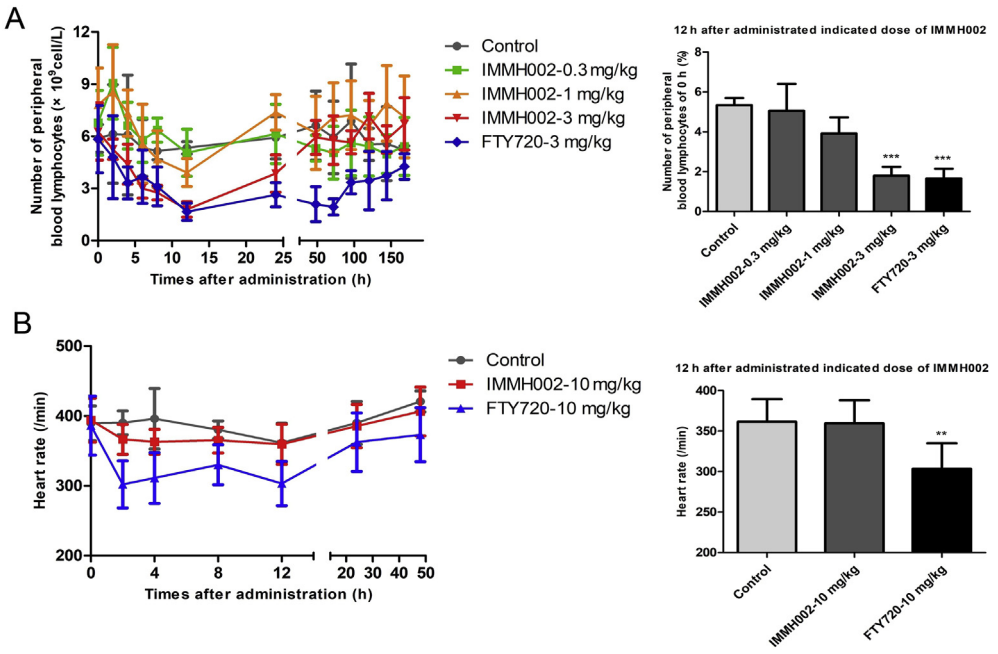

Figure 2 IMMH002 decreases circulating lymphocytes but do not affect heart rate. (A) The number of peripheral blood lymphocytes (PBLs) in SD rats was determined by MEK-7222K type blood cell analyzer at 1, 2, 4, 6, 8, 12, 24, 48, 72, 96, 120, 144 and 168 h post administration with FTY720 and SYL930. Each symbol represents the mean ± SD of 5 animals (left). The percentage of PBL number after 12 h administration of indicated doses of $S1P_1$ agonists to 0 h (right). $^{***}P \leq 0.001$ *vs*. Control. (B) The effect of heart rate followed by $S1P_1$ agonists administration (left manel) and quantification of the heart rate at 12 h (right panel). Heart rate of SD rats was measured at 0, 2, 4, 8, 12, 24 and 48 h post administration of vehicle, 10 mg/kg FTY720 and 10 mg/kg SYL930. Each symbol represents the mean ± SD of 5 animals. $^{**}P \leq 0.01$ *vs*. Control.

0.3, 1 and 3 mg/kg IMMH002 was 25%, 50% and 71% respectively, suggesting a good dose-dependent response. Importantly, the maximal capacity of IMMH002 to decrease PBLs was very close to FTY720 at the same condition (Fig. 2A).

3.4. A single oral administration of IMMH002 has no effect on heart rate of SD rats

Bradycardia is one of the most serious side effects induced by FTY720. To explore whether IMMH002 displayed such similar side effect, the heart rate of SD rats was monitored at 0, 2, 4, 8, 12 and 24 h after a single dose of 10 mg/kg IMMH002. Intriguingly, the heart rate of rats was not affected by 10 mg/kg IMMH002 treatment (Fig. 2B). In contrast, the heart rate of rats administrated with equal dose of FTY720 decreased 22% as early as 2 h after treatment and lasted for 12 h. In conclusion, IMMH002 had no significant effect on heart rate as displayed by FTY720 in SD rats.

3.5. IMMH002 displays significant therapeutic effect on the SDS-induced skin irritation in mice

SDS-induced mouse skin irritation model is a well-established skin irritation model. When the skin is exposed to the aqueous solution of the surfactant SDS, it penetrates into the skin and disrupts this barrier. We therefore used this model to assess whether IMMH002 had therapeutic effect on skin irritation. Normal control KM mice received vehicle treatment (normal control), while animals challenged with 15% SDS for 7 days received vehicle (skin irritation control), 1 mg/kg FTY720, 1.5 mg/kg MTX, and different concentrations of IMMH002 treatment once a day from Day 8 to Day 18. On Day 18, mean skin thickness was determined and pathological assessment was performed. All the treatment groups showed significant improvement compared to the irritation control treated with vehicle. IMMH002 remarkably decreased the skin thickness of mice exposed to SDS and was slightly more effective than FTY720 or MTX (Fig. 3). Importantly, only mice treated with IMMH002 (0.6, 1.2 and 2.4 mg/kg) improved the pathological status despite all compounds ameliorated the skin thickness, indicating that IMMH002 had a potent inhibitory effect on skin inflammation. As the first-line drug used for psoriasis treatment in the clinic, MTX efficiently decreased the thickness of irritated skin, but the body weight started to decline from Day 10, similar effect was also observed in thymus and spleen, which was considered as the adverse effect of MTX treatment (data not shown). Surprisingly, there was no such effect of IMMH002 on the mice body weight, suggesting a safer profile of IMMH002 than MTX.

3.6. IMMH002 has therapeutic effect on psoriasis form skin of guinea pig

We next generated a guinea pig model of psoriasiform skin lesions to evaluate the effect of IMMH002 in a psoriasis model more mimic the human condition. Briefly, a period of 3-week 5% propranolol challenge generated the psoriasiform pathological changes on the ears of guinea pigs. Animals were then orally administered with 0.3, 0.6, 1.2 and 2.4 mg/kg IMMH002, 1.5 mg/kg MTX and 1 mg/kg FTY720 once a day for 2 weeks. Normal control and psoriasis model groups received vehicle treatment only. Intriguingly, IMMH002 attenuated the psoriasiform epidermal changes by decreasing acanthosis, hyperkeratosis, dermal inflammatory infiltration and basilar papilla as well as the thickness of epidermal (Fig. 4A, C, and D). Compared to the psoriasis model group, significant deteriorations were only

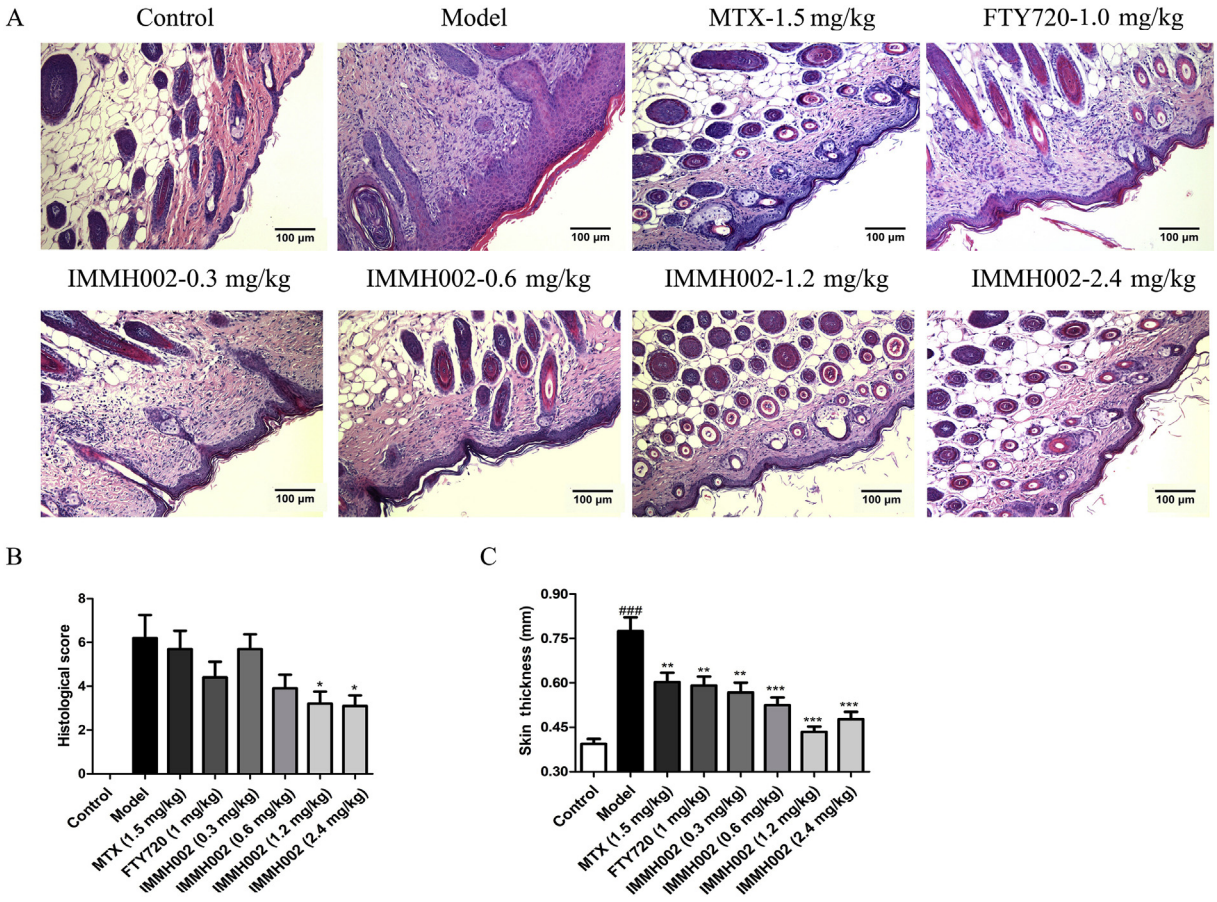

Figure 3 IMMH002 alleviates sodium dodecyl sulphate (SDS)-induced skin irritation in mice ($n = 11$). (A) Representative images of SDS-induced irritation skin of mice treated under various conditions (100 ×). (B) Pathological score of $S1P_1$ agonists and MTX. (C) Skin thickness of irradiation skin of mice. $^{\#\#\#}P \leq 0.001$ *vs.* Control; $^{**}P \leq 0.05$, $^{***}P \leq 0.001$ *vs.* Model.

observed in the 1.2 or 2.4 mg/kg IMMH002, FTY720 and MTX groups. Moreover, IMMH002 could also decrease epidermal PCNA in a dose dependent manner (Fig. 4B and E). Collectively, IMMH002 has a potent therapeutic effect on both skin irritation in mice and psoriasiform skin lesions in guinea pigs with great advantages compared to FTY720 or MTX, indicating IMMH002 represents a potential candidate for the treatment of inflammatory skin disease and psoriasis.

3.7. *IMMH002 relieves skin damage in IMQ-treated mice*

IMQ is a toll-like receptor (TLR) 7/8 agonist which is used for the treatment of actinic keratosis and superficial basal cell carcinoma[29]. However, it also provokes psoriasis-like flares in predisposed patients as an adverse effect. In line with previous reports, we observed that topical application of IMQ on the skin of BALB/c mice induced inflammation with similar features found in psoriatic skin. The PASI score system was applied to evaluate the skin damage, including skin erythema, scaling and thickening. In IMQ-treated mice (IMQ model group), the erythema became detectable on the 3rd day after IMQ treatment (indicated as Day 2 after drug treatment in Fig. 5A). The erythema symptoms developed more severely between Day 3 and Day 5, and then started to recover automatically. The $S1P_1/S1P_3/S1P_4/S1P_5$ agonist FTY720 relieved the erythema only on Day 2 and Day 5, which was similar to MTX. Of note, the more selective $S1P_1$ agonist, IMMH002 ($S1P_1/S1P_4/S1P_5$ agonist), rescued the erythema from Day 2 till the end, especially at the doses of 1.2 and 2.4 mg/kg. The therapeutic effect of IMMH002 on erythema appeared to be superior compared with both FTY720 and MTX. Interestingly, all the treatments could ameliorate the early stage of scaling and skin thickening similarly. As revealed by PASI score analysis, all compounds showed their capacity to improve IMQ-induced skin damage to some extent, while IMMH002 exhibited slight advantages compared to FTY720 and MTX (Fig. 5A).

3.8. *IMMH002 rescues the IMQ-induced pathological skin damage*

IMQ treatment induces different significant pathological change in the skin. For keratose, it causes microabscess, hyperkeratosis and parakeratosis. For epidermis, it mainly induces acanthosis and basilar papilla. And for dermis, inflammatory cells infiltrations, vasodilatation, and thinning above papillae are all observed after IMQ challenge. Treatment of IMMH002 at higher doses (1.2 and 2.4 mg/kg) substantially decreased the pathological damage of all skin layers, and the therapeutic effects were much significant than MTX and FTY720. Acanthosis is the major damage found in psoriasis, so we measured the thickness of epidermis. Our results suggested that all these compounds could relieve the thickening of epidermis, particularly IMMH002 (Fig. 5B and C).

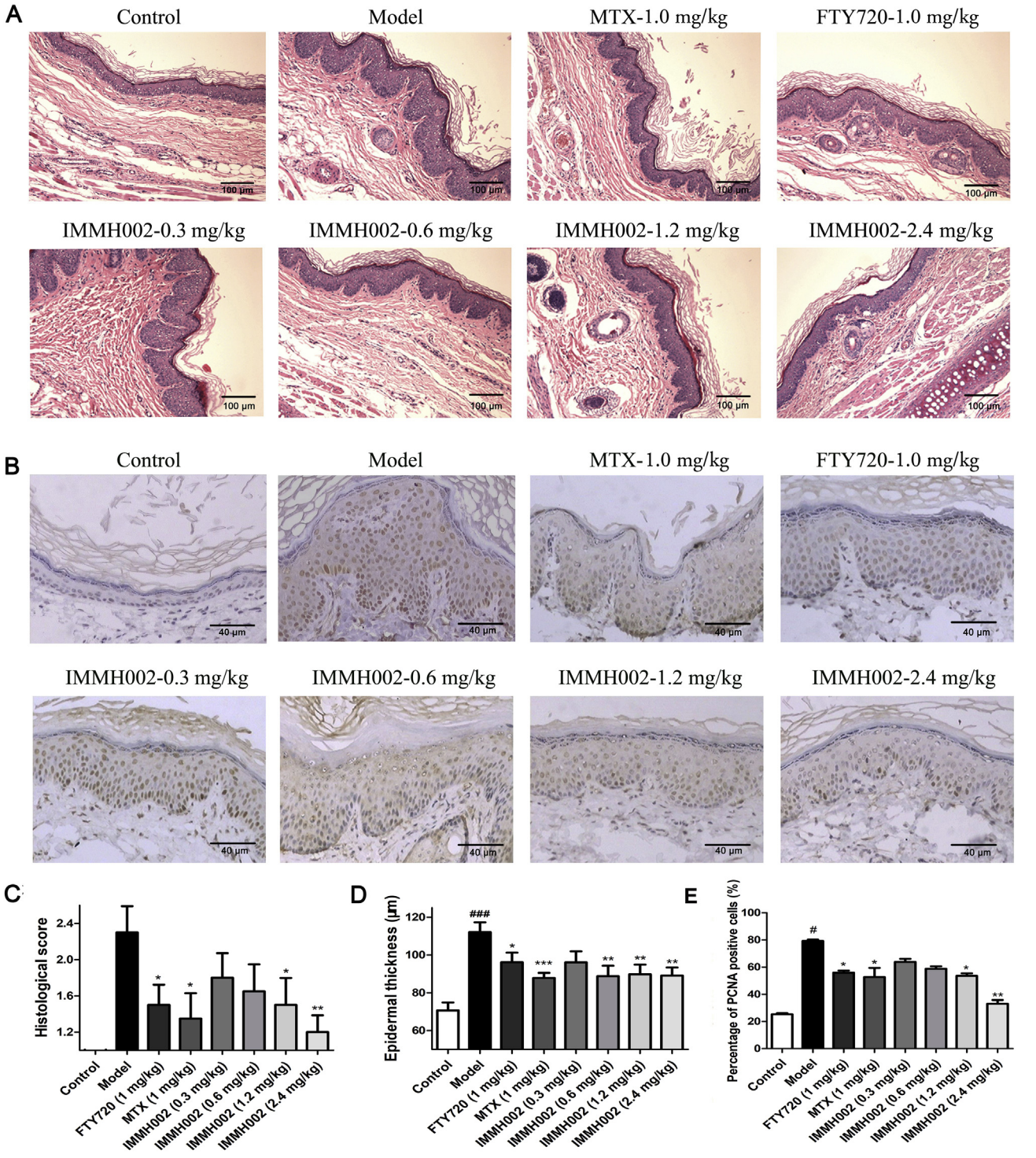

Figure 4 IMMH002 ameliorates propranolol induced psoriasis in guinea pig ($n = 8$). (A) Representative images of HE staining of skin sections from the various groups (100 ×). (B) Representative images of histology and immunohistochemistry of PCNA from the various groups (100 ×). (C) Quantification of histological scoring of HE staining. (D) Epidermal thickness of the skin. (E) Quantification of percentage of PCNA positive cells. $^{###}P<0.001$ *vs*. Control; $^{*}P<0.05$, $^{**}P<0.01$, $^{***}P<0.001$ *vs*. Model.

3.9. IMMH002 decreases T lymphocyte numbers in both the circulating system and psoriasis region

In order to check whether IMMH002 affected lymphocyte homing in IMQ-treated mice, flow cytometry was performed to investigate T cell numbers in the blood, spleen and thymus. The expression of the T cell marker CD3 in skin was also determined by Western blot. In contrast to the IMQ-treated model group, $CD3^+$ T cells were markedly decreased in the blood and spleen, but highly increased in the thymus after IMMH002 treatment, further supporting the essential role of $S1P_1$ in lymphocyte homing (Fig. 6A and B). Moreover, IMQ challenge increased the expression of

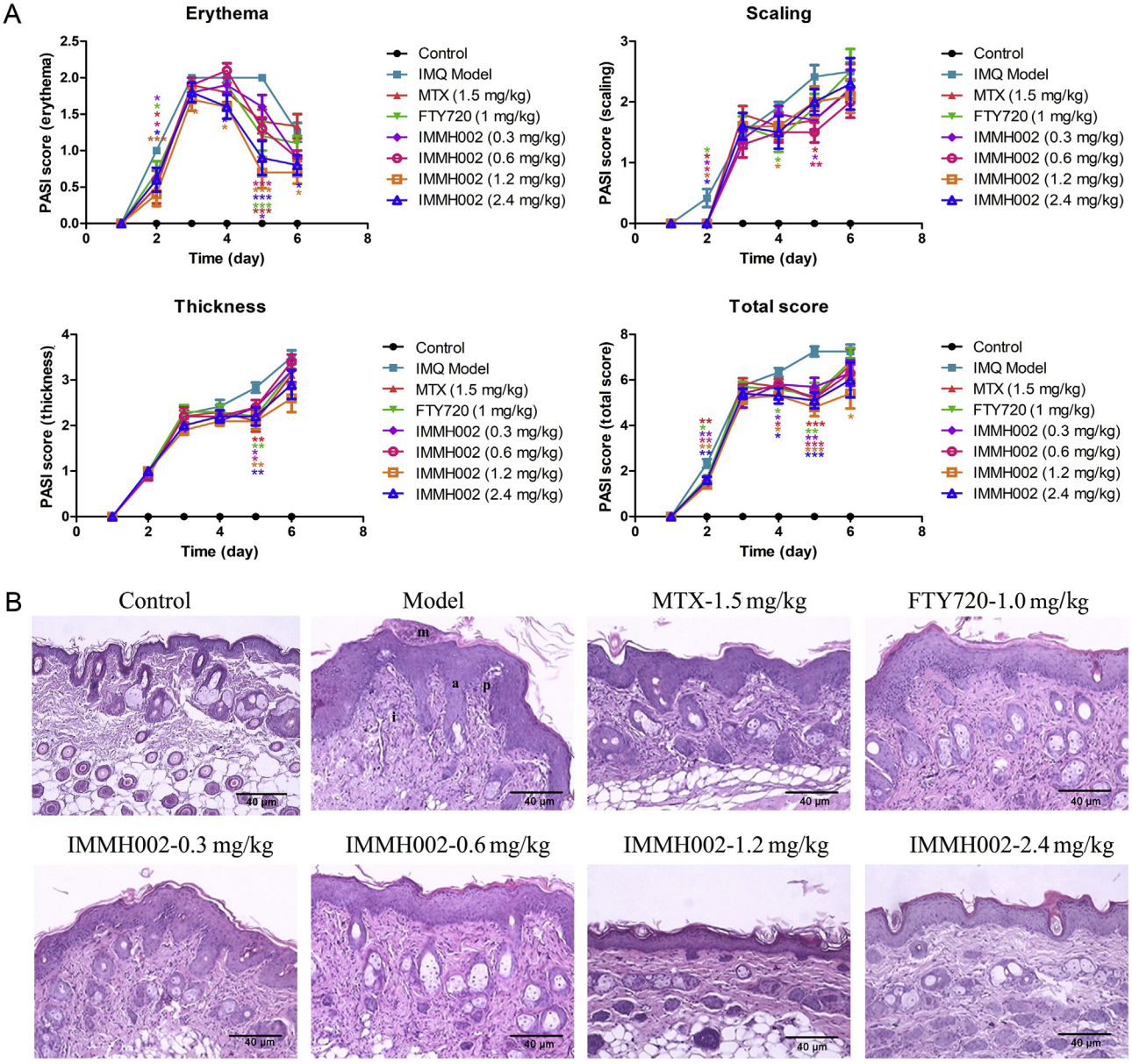

Figure 5 IMMH002 ameliorate IMQ-induced psoriatic symptoms and pathological damage in mice ($n = 10$). (A) Psoriasis area and severity index (PASI) which including erythema, scaling, thickness and total score was applied from Day 1 to Day 6. B. Representative images of psoriasiform lesions in mice back skin with microabscess (m), acanthosis (a), basilar papilla (p) and inflammatory infiltrations (i) (100 ×). Quantification of histological scoring and statistical analysis by ANOVA. (C) Quantification of thickness of acanthosis. $^{*}P \leq 0.05$, $^{**}P \leq 0.01$, $^{***}P \leq 0.001$ *vs*. Model; $^{\#\#\#}P \leq 0.001$ *vs*. Control.

CD3 protein levels in skin legions, whereas IMMH002 could significantly decrease this effect (Fig. 6C and D). Furthermore, protein chip analysis showed that IMMH002 suppressed the expression of the pro-inflammatory cytokines, such as IL17A and IL12p40/p70 in IMQ-dependent psoriasis skin legions (Fig. 7), which might further explain its therapeutic effect in this psoriasis model.

4. Discussion

Psoriasis is a chronic immune system disorder with cutaneous and systemic manifestations, which substantially impairs patients' life qualify. Similar to other autoimmune diseases, lymphocyte infiltration and activation is involved in psoriasis development[30,31]. $S1P_1$ modulators show great beneficial effects on many autoimmune diseases by inducing lymphopenia and preventing tissue inflammation, leading to the development of a new class of targeted therapies for psoriasis. For instance, ponesimod, a selective agonist on $S1P_1$/$S1P_4$/$S1P_5$, has successfully entered a phase-II clinical trial for the treatment of moderate-to-severe chronic plaque psoriasis. It turned out to be of great efficacy, safety and tolerability for psoriasis patients[17].

IMMH002 was first synthesized by the Institute of Materia Medica, Chinese Academy of Medical Sciences & Peking Union Medical College (IMM, CAMS & PUMC, Beijing, China) and the previous study revealed that structural rigidity of the lipophilic chain was required to increase $S1P_1$ agonistic potency and subtype selectivity. Therefore, the chemical structure of IMMH002 was

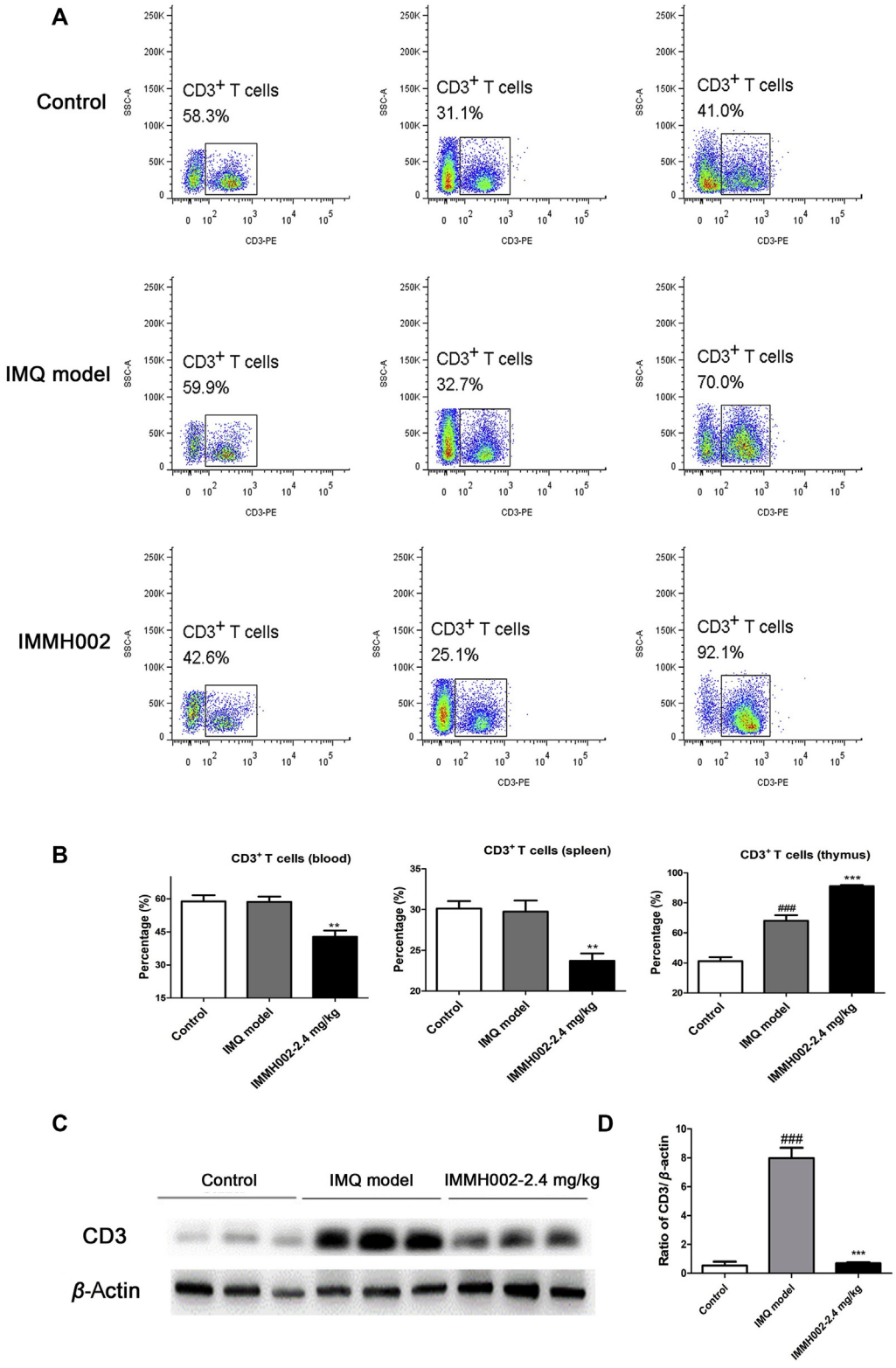

Figure 6 IMMH002 reduces $CD3^+$ T cell skin infiltration in IMQ-challenged mice. (A) Flow cytometry analysis of $CD3^+$ T cell in the blood, spleen and thymus of mice ($n = 4$). (B) The percentage of $CD3^+$ T cell in the blood, spleen and thymus of mice. Statistical analysis was performed by ANOVA. (C) Western blot (WB) test of CD3 protein levels in IMQ-challenged skin. (D) Quantification and statistical analysis of WB result with ANOVA. $^{###}P<0.001$ *vs*. Control; $^{**}P<0.01$, $^{***}P<0.001$ *vs*. Model.

modified according to FTY720 in order to avoid undesired S1P3 activity. The β-arrestin assay indicated that the active form of IMMH002, IMMH002-P, had great agonist activity on $S1P_1$, $S1P_4$ and $S1P_5$, but not $S1P_2$ or $S1P_3$. This specificity excluded its potential side effects such as reduction of heart rate and an increase of blood pressure as reported with FTY720[32]. Moreover, modulation of $S1P_2$ and $S1P_3$ on myofibroblasts by FTY720 also triggered extracellular matrix synthesis, which might contribute to

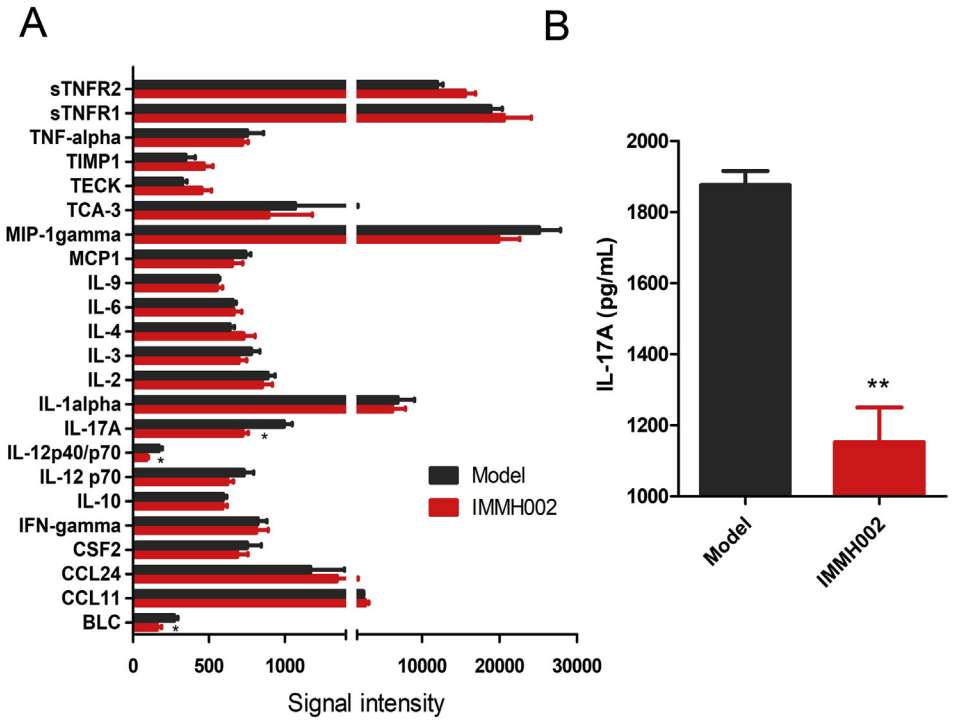

Figure 7 IMMH002 decrease IL17A in IMQ challenged mice skin tested by protein chip. (A) The statistical analysis of protein chip by independent sample *t* test. Each group contains 3 animal skin samples. (B) ELISA assay of IL17A. $^{**}P \leq 0.05$ *vs*. Model.

its adverse side effects in the lung[33–36]. Thus, with higher selectivity, as proved by the *in vivo* studies, IMMH002 might induce less adverse effects than FTY720.

We then investigated the downstream action after $S1P_1$ activation by IMMH002-P. Flow cytometry analysis showed that IMMH002-P decreased the expression of $S1P_1$ on $hS1P_1$-CHO cell membrane. Therefore, after binding and activating $S1P_1$, IMMH002-P caused a temporary $S1P_1$-deficient state, which might render lymphocytes insensitive to the S1P signal necessary for egress from SLO and the thymus. These results were consistent with the mechanisms of other reported $S1P_1$ agonists, such as FTY720 and BAF312[37,38]. In addition, the effect of IMMH002-P on the polyubiquitination and degradation of $S1P_1$ receptors was tested. Interestingly, in contrast to FTY720-P, IMMH002-P did not induce degradation of $S1P_1$ receptors, suggesting different mechanisms to modulate $S1P_1$ turnover between these two compounds (data not shown).

Driven by the exciting *in vitro* data, we investigated the effect of IMMH002 on PBLs. In SD rats, IMMH002 administration resulted in significant lymphopenia in a dose-dependent manner. The maximal lymphopenia efficacy of IMMH002 was similar to FTY720, and both of their maximal efficacies were observed at 12 h post-administration. However, IMMH002-treated rats exhibited a quicker recovery of PBLs suppression, whereas the immunosuppressive effects lasted much longer in the FTY720-treated group. This might be partially explained due to the relatively shorter half-life ($t_{1/2}$) of IMMH002-P (about 11 h) compared to FTY720-P (25 h). The relatively short $t_{1/2}$ of IMMH002 might allow a rapid recovery of blood lymphocyte counts upon deprivation of the treatment and would require daily oral administration in clinical.

The influence of IMMH002 on heart rate in rats was also investigated since bradycardia was one of the most severe adverse effects observed in clinic induced by FTY720 treatment. Our data suggested that single oral administration of SD rats with 10 mg/kg IMMH002 did not affect the heart rate but single oral administration with equal dose of FTY720 indeed caused an immediate 20% heart rate decrease which lasted for 12 h. Previously, studies in rodents revealed that the activation of $S1P_3$ on cardiac myocytes by FTY720 was associated to the reduction of heart rate by stimulating G-protein-coupled inwardly rectifying potassium channels (GIRK), a key player that regulated pacemaker frequency[39]. Intriguingly, Hamada et al.[40] Reported that simple removal of the $S1P_3$ agonist was not sufficient to avoid such cardiovascular side effect in rats. Furthermore, Fryer et al.[41] Suggested that in rats, bradycardia was caused by $S1P_1$ receptor agonist while the increased arterial blood pressure was triggered by $S1P_3$ activation. Importantly, bradycardia in humans was also observed in the recent clinical trials of the $S1P_1/S1P_5$ dual agonist, BAF312. Therefore, whether IMMH002 would cause bradycardia in humans remains unclear. Nevertheless, sparing the $S1P_3$ activation has been still actively proposed as a practical approach to avoid potential side effects. Several more selective $S1P_1$ agonists, such as KRP203, BAF312, CS-0777, ACT128800, ONO-4641, RPC-1063 and MT-1303, have been tested in clinical trials for the treatment of different autoimmune diseases[26,27,42–45].

The etiology of psoriasis is closely correlated with lymphocyte dysregulation. Inspired by the results of ponesimod for psoriasis therapy, the effect of IMMH002 was tested on psoriasis in different animal models.

Skin inflammation is one of the most common and basic characteristics of psoriasis. In order to assess whether IMMH002 could relieve skin inflammation, the SDS-induced skin irritation model was employed. Our data indicate that IMMH002 decreased the pathological score in a dose-dependent manner with a

corresponding reduction in thickness of irritated skin. Although FTY720 and MTX decreased the pathological damage to some extent, it seemed their effect was not as significant as IMMH002. We then used propranolol-induced psoriasiform skin lesions in guinea pig to evaluate the therapeutic effect of IMMH002 on psoriasis. This model mimics the characteristics of epidermal damage in human psoriasis, especially hyperkeratosis, parakeratosis and acanthosis. In addition to the improvement of pathological damage in this model, IMMH002 also decreased the percentage of PCNA in the epidermis, which was closely associated with a reduction of pathological acanthosis.

Consistently, we found that topical application of IMQ on the skin of BALB/c mice induced inflammation with similar features found in psoriatic skin, including formation of microabscesses, skin thickening, hyperkeratosis, acanthosis, scaling and erythema. Orally administration of IMMH002 significantly improved these symptoms and dramatically reduced the PASI score. Notably, T cells, especially T helper (Th) cells producing interleukin (IL)-17, IL-22, and tumor necrosis factor (TNF), form the major T cell population that drive psoriasis pathogenesis. They orchestrate the inflammation in the skin which further induces the proliferation of keratinocytes and endothelial cells. In the IMQ-induced psoriasis model, IMMH002 significantly reduced $CD3^+$ T cells in the skin and blood but increased them in the thymus; furthermore, the key cytokines in psoriasis skin, IL17A and the well-known T cell stimulating factor IL12p40/p70, were also markedly reduced in the IMMH002-treatment group. Previous studies have shown that dendritic cell-induced T cells accumulation is closely related to IMQ-induced mouse psoriasis[46,47]. Thus, dendritic cells (DCs) in the blood were also measured (Supporting Information Fig. S1). There were no significant changes of conventional dendritic cells (cDCs) and plasmacytoid dendritic cells (pDCs) in the blood, but mature DCs were decreased, which were consistent with the reduction of T cells in blood treated with IMMH002. It is indicated that FTY720 could inhibit migration of DCs and function in many inflammatory diseases[48–50]. Similarly, we also found that IMMH002 reduced blood mature DCs. However, whether it could modulate the migration of DCs requires further study.

5. Conclusions

Our study demonstrated that with high selectivity against $S1P_1$, the novel $S1P_1$ modulator IMMH002 could bind and regulate $S1P_1$ expressed on the cell membrane. The active form of IMMH002, IMMH002-P, could effectively decrease the expression of $S1P_1$ by inducing internalization of these receptors, acting as a functional antagonist. MMH002 could remarkably decrease PBLs without obvious adverse effects on heart rate in SD rats and had a good pharmacokinetic profile, especially a relatively short half-life, allowing a quick recover of lymphopenia after the treatment. IMMH002 exhibited significant therapeutic effect on many psoriasis animal models because of its effect on lymphocytes redistribution and infiltration. Based on these above findings, we propose IMMH002 may represent a potential drug candidate for the treatment of psoriasis.

Acknowledgment

This work is supported by the CAMS Innovation Fund for Medical Sciences (2016-I2M-3-008, China), National Natural Science Foundation of China (NSFC Nos. 81872923 and 81473096), Beijing Natural Science Foundation (No. 7172140, China) and The Drug Innovation Major Project (No. 2018ZX09711001-003, China).

Author contributions

Jing Jin and Nina Xue carried out most of the research work. And the manuscript was written by Jing Jin. Yuan Liu, Rong Fu, Mingjin Wang, and Xiaoying Zhang helped carry out the mechanism study. Ming Ji, Fangfang Lai and Jinping Hu helped carry out the animal experiment. Xiaojian Wang, Qiong Xiao and Dali Yin supported the compounds used in this work. Liping Bai did some chemical research of the compounds used in this work. Xiaoguang Chen and Shuan Rao designed the research and revised the paper.

Conflicts of interest

The authors declare no conflicts of interest.

Appendix A. Supporting information

Supporting data to this article can be found online at https://doi.org/10.1016/j.apsb.2019.11.006.

References

1. Greb JE, Goldminz AM, Elder JT, Lebwohl MG, Gladman DD, Wu JJ, et al. Psoriasis. *Nat Rev Dis Primers* 2016;**2**:16082.
2. Rapp SR, Feldman SR, Exum ML, Fleischer Jr AB, Reboussin DM. Psoriasis causes as much disability as other major medical diseases. *J Am Acad Dermatol* 1999;**41**:401–7.
3. Chiricozzi A, Saraceno R, Novelli L, Fida M, Caso F, Scarpa R, et al. Small molecules and antibodies for the treatment of psoriasis: a patent review (2010–2015). *Expert Opin Ther Pat* 2016;**26**:757–66.
4. Rustin MH. Long-term safety of biologics in the treatment of moderate-to-severe plaque psoriasis: review of current data. *Br J Dermatol* 2012;**167 Suppl 3**:3–11.
5. Rizvi S, Chaudhari K, Syed BA. The psoriasis drugs market. *Nat Rev Drug Discov* 2015;**14**:745–6.
6. Rosen H, Gonzalez-Cabrera PJ, Sanna MG, Brown S. Sphingosine 1-phosphate receptor signaling. *Annu Rev Biochem* 2009;**78**:743–68.
7. Kwong E, Li Y, Hylemon PB, Zhou H. Bile acids and sphingosine-1-phosphate receptor 2 in hepatic lipid metabolism. *Acta Pharm Sin B* 2015;**5**:151–7.
8. Chiba K. FTY720, a new class of immunomodulator, inhibits lymphocyte egress from secondary lymphoid tissues and thymus by agonistic activity at sphingosine 1-phosphate receptors. *Pharmacol Ther* 2005;**108**:308–19.
9. Cyster JG. Chemokines, sphingosine-1-phosphate, and cell migration in secondary lymphoid organs. *Annu Rev Immunol* 2005;**23**:127–59.
10. Ogawa E, Sato Y, Minagawa A, Okuyama R. Pathogenesis of psoriasis and development of treatment. *J Dermatol* 2018;**45**:264–72.
11. Malakouti M, Brown GE, Wang E, Koo J, Levin EC. The role of IL-17 in psoriasis. *J Dermatol Treat* 2015;**26**:41–4.
12. AbuHilal M, Walsh S, Shear N. The role of IL-17 in the pathogenesis of psoriasis and update on IL-17 inhibitors for the treatment of plaque psoriasis. *J Cutan Med Surg* 2016;**20**:509–16.
13. Suzuki S, Li XK, Shinomiya T, Enosawa S, Amemiya H, Amari M, et al. The *in vivo* induction of lymphocyte apoptosis in MRL-*lpr/lpr* mice treated with FTY720. *Clin Exp Immunol* 1997;**107**:103–11.
14. Matsuura M, Imayoshi T, Chiba K, Okumoto T. Effect of FTY720, a novel immunosuppressant, on adjuvant-induced arthritis in rats. *Inflamm Res* 2000;**49**:404–10.

15. Chun J, Hartung HP. Mechanism of action of oral fingolimod (FTY720) in multiple sclerosis. *Clin Neuropharmacol* 2010;**33**:91−101.
16. Brinkmann V, Billich A, Baumruker T, Heining P, Schmouder R, Francis G, et al. Fingolimod (FTY720): discovery and development of an oral drug to treat multiple sclerosis. *Nat Rev Drug Discov* 2010;**9**:883−97.
17. Vaclavkova A, Chimenti S, Arenberger P, Holló P, Sator PG, Burcklen M, et al. Oral ponesimod in patients with chronic plaque psoriasis: a randomised, double-blind, placebo-controlled phase 2 trial. *The Lancet* 2014;**384**:2036−45.
18. Ryan C, Menter A. Ponesimod—a future oral therapy for psoriasis?. *The Lancet* 2014;**384**:2006−8.
19. Ji M, Xue N, Lai F, Zhang X, Zhang S, Wang Y, et al. Validating a selective $S1P_1$ receptor modulator Syl930 for psoriasis treatment. *Biol Pharm Bull* 2018;**41**:592−6.
20. Tian Y, Jin J, Wang X, Hu J, Xiao Q, Zhou W, et al. Discovery of oxazole and triazole derivatives as potent and selective $S1P_1$ agonists through pharmacophore-guided design. *Eur J Med Chem* 2014;**85**:1−15.
21. Mi J, Zhao M, Yang S, Yang S, Jin J, Wang X, et al. Pharmacokinetics of H002, a novel S1PR1 modulator, and its metabolites in rat blood using liquid chromatography-tandem mass spectrometry. *Acta Pharm Sin B* 2016;**6**:576−83.
22. Tian Y, Jin J, Wang X, Han W, Li G, Zhou W, et al. Design, synthesis and docking-based 3D-QSAR study of novel 2-substituted 2-aminopropane-1,3-diols as potent and selective agonists of sphingosine-1-phosphate 1 ($S1P_1$) receptor. *MedChemComm* 2013;**4**:1267.
23. Talmadge JE, Jackson JD, Borgeson CD, Perry GA. Differential recovery of polymorphonuclear neutrophils, B and T cell subpopulations in the thymus, bone marrow, spleen and blood of mice following split-dose polychemotherapy. *Cancer Immunol Immunother* 1994;**39**:59−67.
24. Wang H, Jiang M, Cui H, Chen M, Buttyan R, Hayward SW, et al. The stress response mediator ATF3 represses androgen signaling by binding the androgen receptor. *Mol Cell Biol* 2012;**32**:3190−202.
25. Jin J, Hu J, Zhou W, Wang X, Xiao Q, Xue N, et al. Development of a selective $S1P_1$ receptor agonist, Syl930, as a potential therapeutic agent for autoimmune encephalitis. *Biochem Pharmacol* 2014;**90**:50−61.
26. Shimizu H, Takahashi M, Kaneko T, Murakami T, Hakamata Y, Kudou S, et al. KRP-203, a novel synthetic immunosuppressant, prolongs graft survival and attenuates chronic rejection in rat skin and heart allografts. *Circulation* 2005;**111**:222−9.
27. Bolli MH, Abele S, Binkert C, Bravo R, Buchmann S, Bur D, et al. 2-Imino-thiazolidin-4-one derivatives as potent, orally active $S1P_1$ receptor agonists. *J Med Chem* 2010;**53**:4198−211.
28. Marsolais D, Rosen H. Chemical modulators of sphingosine-1-phosphate receptors as barrier-oriented therapeutic molecules. *Nat Rev Drug Discov* 2009;**8**:297−307.
29. Telo I, Pescina S, Padula C, Santi P, Nicoli S. Mechanisms of imiquimod skin penetration. *Int J Pharm* 2016;**511**:516−23.
30. Hawkes JE, Chan TC, Krueger JG. Psoriasis pathogenesis and the development of novel targeted immune therapies. *J Allergy Clin Immunol* 2017;**140**:645−53.
31. Diani M, Altomare G, Reali E. T helper cell subsets in clinical manifestations of psoriasis. *J Immunol Res* 2016;**2016**:7692024.
32. Forrest M, Sun SY, Hajdu R, Bergstrom J, Card D, Doherty G, et al. Immune cell regulation and cardiovascular effects of sphingosine 1-phosphate receptor agonists in rodents are mediated *via* distinct receptor subtypes. *J Pharmacol Exp Ther* 2004;**309**:758−68.
33. Milara J, Navarro R, Juan G, Peiro T, Serrano A, Ramon M, et al. Sphingosine-1-phosphate is increased in patients with idiopathic pulmonary fibrosis and mediates epithelial to mesenchymal transition. *Thorax* 2012;**67**:147−56.
34. Murakami K, Kohno M, Kadoya M, Nagahara H, Fujii W, Seno T, et al. Knock out of $S1P_3$ receptor signaling attenuates inflammation and fibrosis in bleomycin-induced lung injury mice model. *PLoS One* 2014;**9**. e106792.
35. Gendron DR, Lemay AM, Lecours PB, Perreault-Vallieres V, Huppe CA, Bosse Y, et al. FTY720 promotes pulmonary fibrosis when administered during the remodelling phase following a bleomycin-induced lung injury. *Pulm Pharmacol Ther* 2017;**44**:50−6.
36. Oo ML, Chang SH, Thangada S, Wu MT, Rezaul K, Blaho V, et al. Engagement of $S1P_1$-degradative mechanisms leads to vascular leak in mice. *J Clin Investig* 2011;**121**:2290−300.
37. Gergely P, Nuesslein-Hildesheim B, Guerini D, Brinkmann V, Traebert M, Bruns C, et al. The selective sphingosine 1-phosphate receptor modulator BAF312 redirects lymphocyte distribution and has species-specific effects on heart rate. *Br J Pharmacol* 2012;**167**:1035−47.
38. Mandala S, Hajdu R, Bergstrom J, Quackenbush E, Xie J, Milligan J, et al. Alteration of lymphocyte trafficking by sphingosine-1-phosphate receptor agonists. *Science* 2002;**296**:346−9.
39. Koyrakh L, Roman MI, Brinkmann V, Wickman K. The heart rate decrease caused by acute FTY720 administration is mediated by the G protein-gated potassium channel I. *Am J Transplant* 2005;**5**:529−36.
40. Hamada M, Nakamura M, Kiuchi M, Marukawa K, Tomatsu A, Shimano K, et al. Removal of sphingosine 1-phosphate receptor-3 ($S1P_3$) agonism is essential, but inadequate to obtain immunomodulating 2-aminopropane-1,3-diol $S1P_1$ agonists with reduced effect on heart rate. *J Med Chem* 2010;**53**:3154−68.
41. Fryer RM, Muthukumarana A, Harrison PC, Nodop Mazurek S, Chen RR, Harrington KE, et al. The clinically-tested S1P receptor agonists, FTY720 and BAF312, demonstrate subtype-specific bradycardia ($S1P_1$) and hypertension ($S1P_3$) in rat. *PLoS One* 2012;**7**. e52985.
42. Pan S, Gray NS, Gao W, Mi Y, Fan Y, Wang X, et al. Discovery of BAF312 (siponimod), a potent and selective S1P receptor modulator. *ACS Med Chem Lett* 2013;**4**:333−7.
43. Nishi T, Miyazaki S, Takemoto T, Suzuki K, Iio Y, Nakajima K, et al. Discovery of CS-0777: a potent, selective, and orally active $S1P_1$ agonist. *ACS Med Chem Lett* 2011;**2**:368−72.
44. Komiya T, Sato K, Shioya H, Inagaki Y, Hagiya H, Kozaki R, et al. Efficacy and immunomodulatory actions of ONO-4641, a novel selective agonist for sphingosine 1-phosphate receptors 1 and 5, in preclinical models of multiple sclerosis. *Clin Exp Immunol* 2013;**171**:54−62.
45. Taylor Meadows KR, Steinberg MW, Clemons B, Stokes ME, Opiteck GJ, Peach R, et al. Ozanimod (RPC1063), a selective $S1PR_1$ and $S1PR_5$ modulator, reduces chronic inflammation and alleviates kidney pathology in murine systemic lupus erythematosus. *PLoS One* 2018;**13**. e0193236.
46. Ueyama A, Yamamoto M, Tsujii K, Furue Y, Imura C, Shichijo M, et al. Mechanism of pathogenesis of imiquimod-induced skin inflammation in the mouse: a role for interferon-alpha in dendritic cell activation by imiquimod. *J Dermatol* 2014;**41**:135−43.
47. Takagi H, Arimura K, Uto T, Fukaya T, Nakamura T, Choijookhuu N, et al. Plasmacytoid dendritic cells orchestrate TLR7-mediated innate and adaptive immunity for the initiation of autoimmune inflammation. *Sci Rep* 2016;**6**:24477.
48. Han Y, Li X, Zhou Q, Jie H, Lao X, Han J, et al. FTY720 abrogates collagen-induced arthritis by hindering dendritic cell migration to local lymph nodes. *J Immunol* 2015;**195**:4126−35.
49. Idzko M, Hammad H, van Nimwegen M, Kool M, Müller T, Soullié T, et al. Local application of FTY720 to the lung abrogates experimental asthma by altering dendritic cell function. *J Clin Investig* 2006;**116**:2935−44.
50. Lan YY, De Creus A, Colvin BL, Abe M, Brinkmann V, Coates PT, et al. The sphingosine-1-phosphate receptor agonist FTY720 modulates dendritic cell trafficking *in vivo*. *Am J Transplant* 2005;**5**:2649−59.